

Model of the double-rotor induction motor in terms of electromagnetic differential

DOMINIK ADAMCZYK, ANDRZEJ WILK, MICHAŁ MICHNA

*Gdansk University of Technology
Faculty of Electrical and Control Engineering
80-233 Gdańsk, ul. Narutowicza 11/12, Poland
e-mail: dadamc@ely.pg.gda.pl, {andrzej.wilk/michal.michna}@pg.gda.pl*

(Received: 25.11.2015, revised: 08.09.2016)

Abstract: The paper presents a concept, a construction, a circuit model and experimental results of the double-rotor induction motor. This type of a motor is to be implemented in the concept of the electromagnetic differential. At the same time it should fulfill the function of differential mechanism and the vehicle drive. One of the motor shafts is coupled to the direction changing mechanical transmission. The windings of the external rotor are powered by slip rings and brushes. The inner rotor has the squirrel-cage windings. The circuit model parameters were calculated based on the 7.5 kW real single-rotor induction motor ($2p = 4$). Experimental verification of the model was based on comparison between the mentioned single-rotor motor and double-rotor model with the outer rotor blocked. The presented results showed relatively good compliance between the model and real motor.

Key words: double rotor, electromagnetic differential, induction machine

1. Introduction

In recent years, some car manufactures started the production and sale of electrical vehicles (EV) in which this kind of a car has an electrical motor as a main drive system. Numerous scientific papers were published about the drive system topology and types of an electrical motor used in EV [1, 2].

Nowadays drive systems in use are based on a single motor drive transmission with a mechanical differential (MD) gear. The multi-motor drive systems (in-wheel hub motor) are less frequently in use. In a multi-motor drive system the differential function is implemented in an electronic master controller. The idea of the electromagnetic differential (EMD) is presented in this paper [12]. The double rotor machine (DRM) can be applied as a mechanical differential gear. It is possible to make EMD using a synchronous machine (SM) or an induction machine (IM).

Nowadays most published papers about double rotor motors present the motor structure with the wound stator and two rotors: inner and outer stator at the center [10, 11]. The rotors are separated from stator by two air gaps. The double rotor induction machine presented in this paper has only one air gap and two rotors (wound and cage) and does not have the wound stator. That is why the main purpose of this paper is to present a mathematical model of the induction motor with two rotors in terms of EMD and analysis of the dynamic properties of this machine. Chapter 2 describes the design and function of the MD. In Chapter 3 the structure of the cage IM as an EMD is showed. Chapter 4 describes a mathematical model of the double rotor IM. The selected results of the dynamic simulations are shown in Chapter 5.

2. Mechanical differential

The mechanical differential provides the ability to vary the speed of rotation for a vehicle drive. This is particularly important when the vehicle turns and one of the drive wheels must overcome a longer distance. MD splits the drive torque of the motor on two drive shafts wheels (theoretically even). At the same time the power is also distributed (divided): the greater to the faster rotating wheel. In some situations, the power/torque distribution can be disadvantageous, eg. when one wheel loses contact with the ground. Therefore, various concepts are developed starting from the MD with increased internal friction (eg. with hydraulic clutch) to the active MD (ie. multi-motor systems) [3]. These solutions allow to arbitrarily distribute torque to each drive shaft. There are also systems in use that are a combination of the MD and braking system. Despite the differences in performance, features and construction the basic function and operating principle of the MD remains unchanged. This paper presents the design, principle of operation and the elementary kinematic and dynamic relationships of the simple MD. Description refers to the bevel gear, the construction of which is shown in Fig. 1.

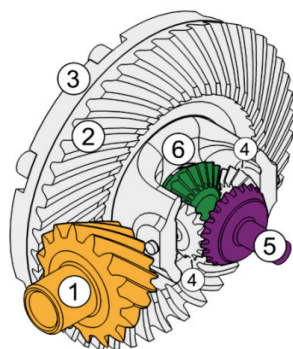


Fig. 1. The mechanical differential (bevel gear): 1-the drive shaft pinion, 2-wheel disc, 3-housing connected to the packing wheel, 4-satellites connected to the housing, 5 and 6 ring/crown gears connected to the drive shaft which drives the wheels

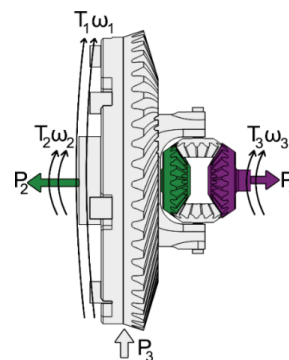


Fig. 2. Marking moments, powers and speeds of the MD individual elements from Fig. 1

The considered system is symmetrical, which means that the number of teeth in both crown wheels is equal. It follows that such a gearbox has an internal gear ratio $i = -1$. The torques, powers and speeds of the MD individual elements is marked in Fig. 2.

The differential transmits the drive torque T_1 from the wheel disc via satellite to the crown gears (T_2, T_3 – driveshaft torque). The torque equation in the MD is as follows:

$$0.5 T_1 = T_2 = T_3. \quad (1)$$

The angular velocity relationship in the MD is expressed by the formula:

$$\omega_1 = (\omega_2 + \omega_3) / 2. \quad (2)$$

The MD power balance (neglecting losses) is:

$$\omega_1 T_1 = (\omega_2 T_2 + \omega_3 T_3) / 2. \quad (3)$$

The torques T_2 and T_3 are the load torques of the drive shafts. On the basis of the Eq. (2) it can be noticed that in the case of blocking one of the drive shafts, the other wheel will rotate at the twice the speed compared to that of the disc wheel. The same situation would occur if one of the wheels lost its grip.

3. The concept/idea of the double-rotor induction motor

The issues concerning a double-rotor induction machine are presented among others in [4, 5].

Fig. 3 shows the design concept of the double-rotor induction motor.

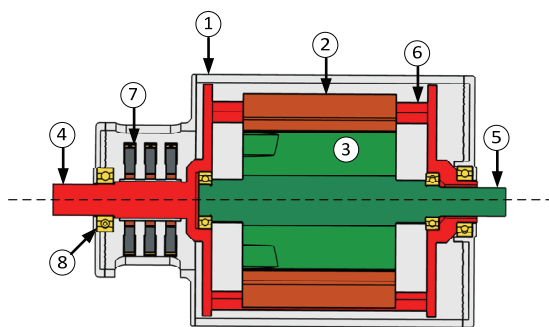


Fig. 3. The design concept of the double-rotor induction motor. 1-non rotating housing, 2-outer rotor yoke, 3-inner rotor yoke, 4-outer rotor shaft, 5-inner rotor shaft, 6-rotating frame of the outer rotor, 7-slip rings and brushes, 8-bearing

The main dimensions of the motor have been calculated on the basis of cage motor type Sg132M4, with nominal power $P_n = 7.5$ kW, the number of pole pairs $p = 2$, the number of stator slots $Q_s = 36$, and the number of rotor slots $Q_r = 28$. In the proposed concept the three-

phase power is supplied to the outer rotor coil windings by the slip ring contact. The full power slip rings and brush power transmission system is a strong drawback of this solution. Unfortunately other methods which allow transmitting power to the rotating winding also provide a number of construction problems.

The inner rotor contains a squirrel-cage winding. The rotating frame of the outer rotor is mounted in bearings embedded in the motor housing. The inner rotor is mounted in bearings embedded in this rotating frame. Hereby achieved the possibility of independent rotation of each of the shafts (rotors). The inner rotor shaft is connected to a mechanical transmission changing the direction of rotation by a sleeve made in the rotating frame. The change of the rotation direction is necessary if the motor will be designed to work as EMD.

4. Mathematical model of the double-rotor induction motor

To obtain the presented mathematical model certain simplifying assumptions have been made:

- 1) Magnetic circuit is linear.
- 2) The only drop of the magneto-motive force is across the air gap.
- 3) The thickness of the air gap is constant.
- 4) Maxwell's equations apply only to a radial component of the magnetic field and induction, while the rest of the components are equal to zero

The mathematical model of the double-rotor induction motor is defined in a natural reference frame. In the case of the considered machine the three phase coil windings of the outer rotor is represented by the three delta connected concentrated windings (Fig. 4).

In the presented model, the only important simplified assumption is about linear magnetic coupling between the outer rotor concentrated windings and the inner rotor cage windings (meshes). The displacement current in the rotor cage bars was taken into account by amending their resistance as a function of the slip.

The hysteresis and eddy current power losses in the conceptual approach have been omitted. The mathematical model of the double rotor machines was formulated using the Lagrange energy method (Lagrange equations). A detailed description of the methodology for modelling induction machines using Lagrange equations is given in [8-9]. The first step, to develop a machine circuit model, is to divide it into lumped conservative and dissipative elements, both electrical and mechanical.

The schematic diagram shown in Fig. 4 includes the lumped elements of the rotating outer coil winding (coils M_{aa} , M_{bb} , M_{cc} and resistors R_{aa} , R_{bb} , R_{cc}).

The motor electromagnetic circuit has three degrees of freedom on the outer rotor side (currents i_a , i_b , i_c) and twenty nine degrees of freedom on the inner rotor side (currents i_{r0}, \dots, i_{r27} , i_e). The motor model complements the mechanical circuit consisting of two inertia elements and two rotational damping elements. In this circuit there are two degrees of freedom: outer rotor angular velocity ω_s and inner rotor angular velocity ω_r .

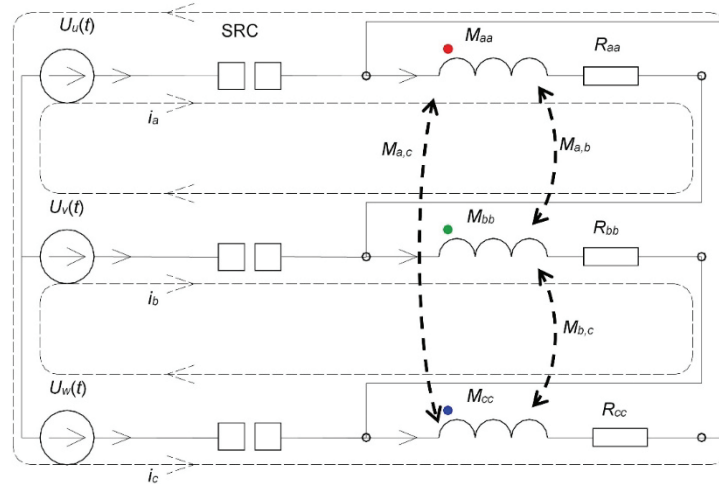


Fig. 4. The schematic diagram of the outer rotor electric circuit: SRC-slip ring contact

The schematic diagram of $\frac{1}{4}$ of the rotor cage is shown in Fig. 5 with the dissipative elements: resistances of bars R_p and rings R_e .

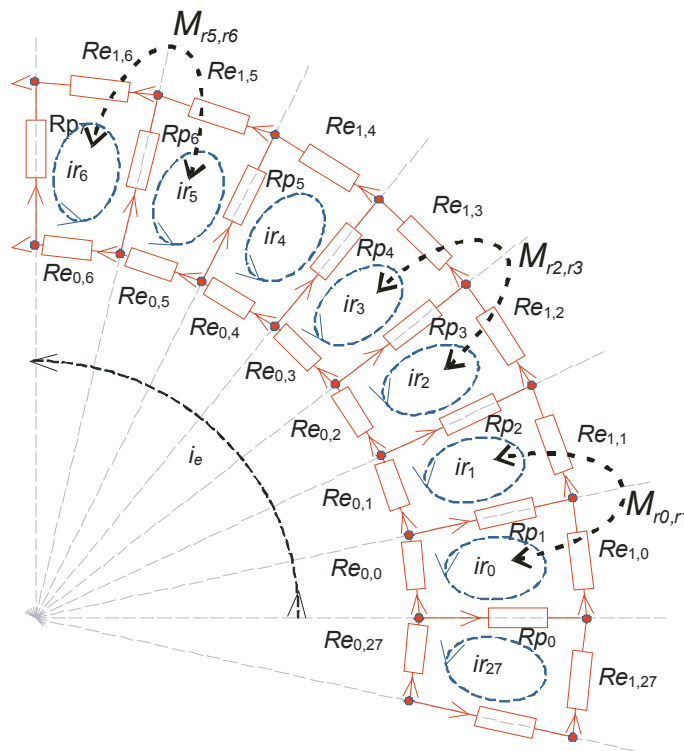


Fig. 5. The schematic diagram of $\frac{1}{4}$ of the rotor cage

The model equations of the double-rotor induction motor are as follow:

$$\begin{aligned}
 \mathbf{M}(\alpha_s, \alpha_r) \frac{d}{dt} \begin{bmatrix} i_a \\ i_b \\ i_c \\ ir_0 \\ \vdots \\ ir_{27} \\ ie \end{bmatrix} &= \begin{bmatrix} U_u(t) - U_v(t) \\ U_v(t) - U_w(t) \\ U_w(t) - U_u(t) \\ 0 \\ \vdots \\ 0 \\ 0 \end{bmatrix} - \mathbf{R}(s) \begin{bmatrix} i_a \\ i_b \\ i_c \\ ir_0 \\ \vdots \\ ir_{27} \\ ie \end{bmatrix} + \\
 - \left[\frac{\partial}{\partial \alpha_s} \mathbf{M}(\alpha_s, \alpha_r) \right] \begin{bmatrix} i_a \\ i_b \\ i_c \\ ir_0 \\ \vdots \\ ir_{27} \\ ie \end{bmatrix} \omega_s - \left[\frac{\partial}{\partial \alpha_r} \mathbf{M}(\alpha_s, \alpha_r) \right] \begin{bmatrix} i_a \\ i_b \\ i_c \\ ir_0 \\ \vdots \\ ir_{27} \\ ie \end{bmatrix} \omega_r.
 \end{aligned} \tag{4}$$

$$\begin{aligned}
 \frac{d}{dt} \alpha_s &= \omega_s, \quad \frac{d}{dt} \alpha_r = \omega_r, \\
 J_s \frac{d}{dt} \omega_s &= T_{\text{elem}_s}(\mathbf{i}, \alpha_s, \alpha_r) + T_{\text{ext}_s}(t) - D_s \omega_s, \\
 J_r \frac{d}{dt} \omega_r &= T_{\text{elem}_r}(\mathbf{i}, \alpha_s, \alpha_r) + T_{\text{ext}_r}(t) - D_r \omega_r.
 \end{aligned} \tag{5}$$

where: α_s is the rotation angle of the outer rotor, α_r is the rotation angle of the inner rotor, $\mathbf{M}(\alpha_s, \alpha_r)$ is an inductance matrix, $\mathbf{R}(s)$ is a resistance matrix as a function of the slip s , J_s , J_r are inertia moments of the outer and inner rotors; $T_{\text{elem}_s}(\mathbf{i}, \alpha_s, \alpha_r)$, $T_{\text{elem}_r}(\mathbf{i}, \alpha_s, \alpha_r)$ are electromagnetic torques acting on the outer and inner rotors; $T_{\text{ext}_s}(t)$, $T_{\text{ext}_r}(t)$ are external loads acting on the outer and inner rotor shafts; D_s , D_r are the kinetic damping coefficient of the outer and inner rotors.

Electromagnetic moments are determined by formula:

$$\begin{aligned}
 T_{\text{elem}_s}(\mathbf{i}, \alpha_s, \alpha_r) &= \frac{1}{2} \mathbf{i}^T \left[\frac{\partial}{\partial \alpha_s} \mathbf{M}(\alpha_s, \alpha_r) \right] \mathbf{i}, \\
 T_{\text{elem}_r}(\mathbf{i}, \alpha_s, \alpha_r) &= \frac{1}{2} \mathbf{i}^T \left[\frac{\partial}{\partial \alpha_r} \mathbf{M}(\alpha_s, \alpha_r) \right] \mathbf{i}, \\
 \mathbf{i}^T &= [i_a \quad i_b \quad i_c \quad ir_0 \quad \cdots \quad ir_{27} \quad i_e].
 \end{aligned} \tag{6}$$

An inductance matrix is given by:

$$\mathbf{M}(\alpha_s, \alpha_r) = \begin{bmatrix} M_{a,a} & M_{a,b} & M_{a,c} & M_{a,r0}(\alpha_s, \alpha_r) & \cdots & M_{a,r27}(\alpha_s, \alpha_r) & 0 \\ M_{b,a} & M_{b,b} & M_{b,c} & M_{b,r0}(\alpha_s, \alpha_r) & \cdots & M_{b,r27}(\alpha_s, \alpha_r) & 0 \\ M_{c,a} & M_{c,b} & M_{c,c} & M_{c,r0}(\alpha_s, \alpha_r) & \cdots & M_{c,r27}(\alpha_s, \alpha_r) & 0 \\ M_{r0,a}(\alpha_s, \alpha_r) & M_{r0,b}(\alpha_s, \alpha_r) & M_{r0,c}(\alpha_s, \alpha_r) & M_{r0,r0} & \cdots & M_{r0,r27r} & 0 \\ \vdots & \vdots & \vdots & \vdots & \ddots & \vdots & \vdots \\ M_{r27,a}(\alpha_s, \alpha_r) & M_{r27,b}(\alpha_s, \alpha_r) & M_{r27,c}(\alpha_s, \alpha_r) & M_{r27,r0} & \cdots & M_{r27,r27} & 0 \\ 0 & 0 & 0 & 0 & \cdots & 0 & M_{e,e} \end{bmatrix} \quad (7)$$

It contains the constant elements $M_{s,s}$ between inductances in the outer rotor circuit and constant elements $M_{r,r}$ in the inner rotor circuit (cage). Self-inductances were increased by $k_{ss} = 1.02$, and $k_{rr} = 1.02$ factor in order to take into account leakages inductances of the coils. The mutual inductances $M_{r,s}$ $M_{s,r}$ between outer and inner rotor circuits are functions of angles α_s , α_r . The angles α_s , α_r were defined with respect to the housing (natural frame). Fig. 6 shows the beginning of two reference frames (outer rotor and inner rotor) and a natural frame. β_{s0} is the beginning of the outer rotor frame, β_{r0} is the beginning of the inner rotor frame, β_0 is the beginning of the natural frame.

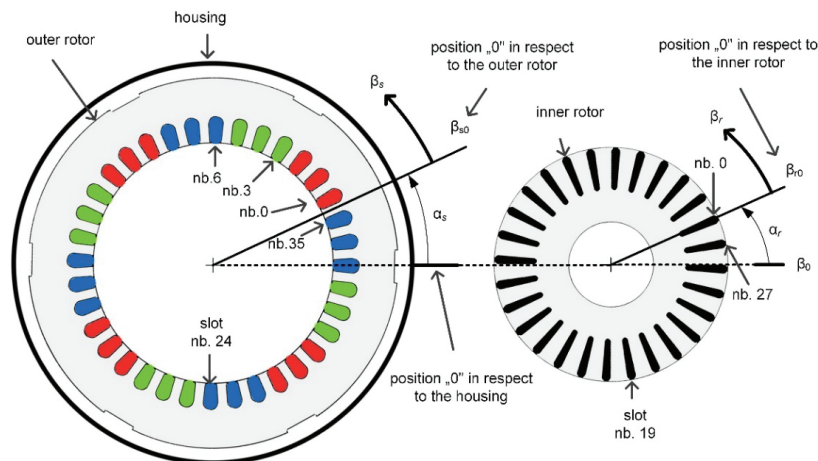


Fig. 6. Definition of axis for inner and outer rotor with respect to the housing

Self and mutual inductances were calculated based on flux distribution caused by current flowing in the phase of the outer rotor or the coil of the inner rotor. Flux distribution is a step function. Fig. 7 shows the flux distribution in an air gap from current flowing in the phase “a” of the outer rotor $B_{s,a}$ for $\alpha_s = 0$. Also an approximation $B_{s,a \text{ harm}}$ of $B_{s,a}$ into 5-th order Fourier series is presented.

The graphs of the mutual inductance as a function of both the angles have been shown in Fig. 8 and Fig. 9.

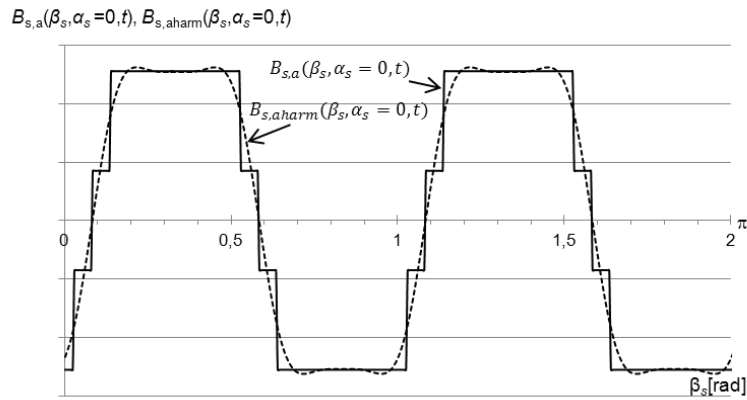


Fig. 7. Flux distribution from current flowing in phase “a” of outer rotor $B_{s,a}(\beta_s, \alpha_s, t)$ and it's approximation in 5-th order furrier series $B_{s,a,harm}(\beta_s, \alpha_s, t)$ for $\alpha_s = 0$ and $\beta_s = 0 \dots 2\pi$

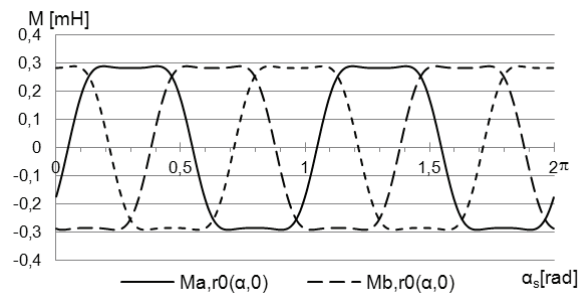


Fig. 8. The graphs of the mutual inductance $M_{a,r0}(\alpha_s, \alpha_r = 0)$, $M_{b,r0}(\alpha_s, \alpha_r = 0)$, $M_{c,r0}(\alpha_s, \alpha_r = 0)$ of the individual outer rotor phases with the inner rotor coil mesh r_0 for angle $\alpha_s = 0 \dots 2\pi$

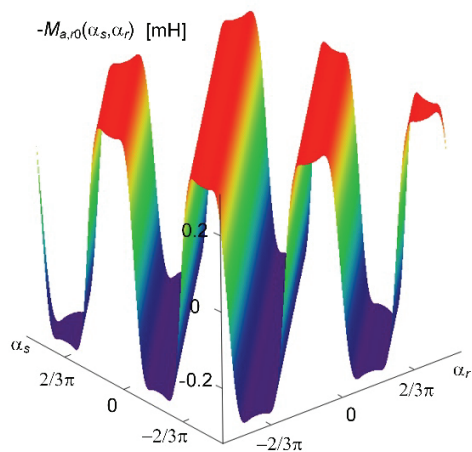


Fig. 9. The graph of the mutual inductance $M_{a,r0}(\alpha_s, \alpha_r)$ between outer phase “a” and inner rotor mesh r_0 for angle $\alpha_s = -\pi \dots \pi$, $\alpha_r = -\pi \dots \pi$

5. Selected results of dynamic simulation

A comparison of the simulation and experiment results was carried out for the motors that, in their starting state, contained a stalled outer rotor. The simulation model was developed in the Synopsys SABER software using the MAST modelling language.

The results of the supply of the current waveform i_a obtained by simulation and experiment has been shown in Fig. 10.

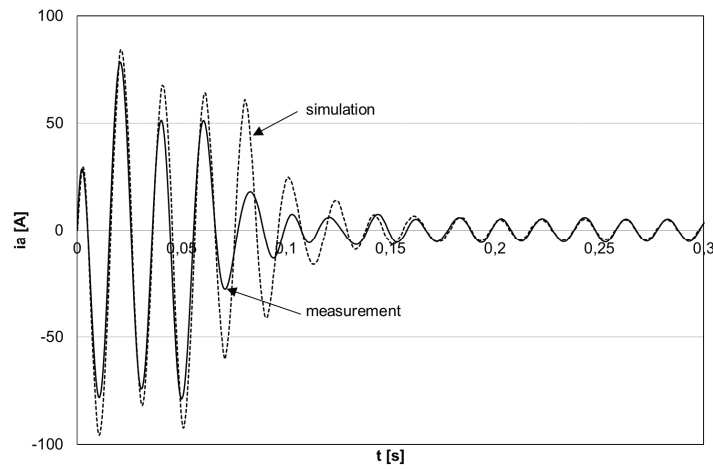


Fig. 10. The comparison of the supply current waveform i_a obtained by simulation (dotted line) and experiment (continues line)

The simulation of electromagnetic torque acting on the inner rotor and its angular velocity during start-up (Fig. 10) has been shown in Fig. 11.

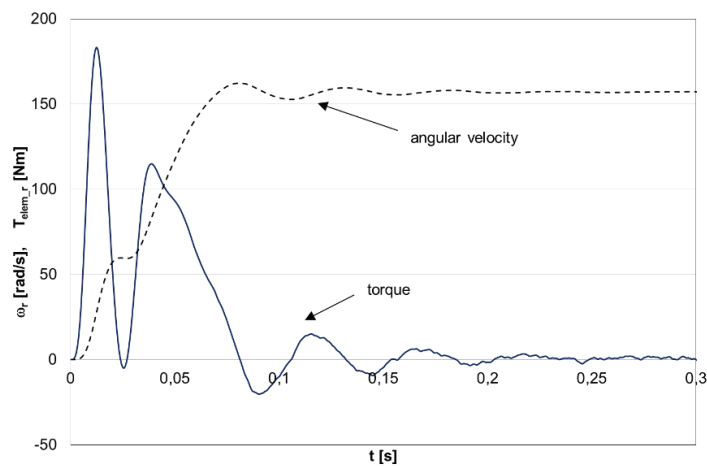


Fig. 11. The simulation of electromagnetic torque acting on the inner rotor and its angular velocity

Based on these results it can be concluded that the model reasonably well reproduces the results obtained from the experiments. Fig. 12 and Fig. 13 are showing the results of start-up simulations with two rotating rotors.

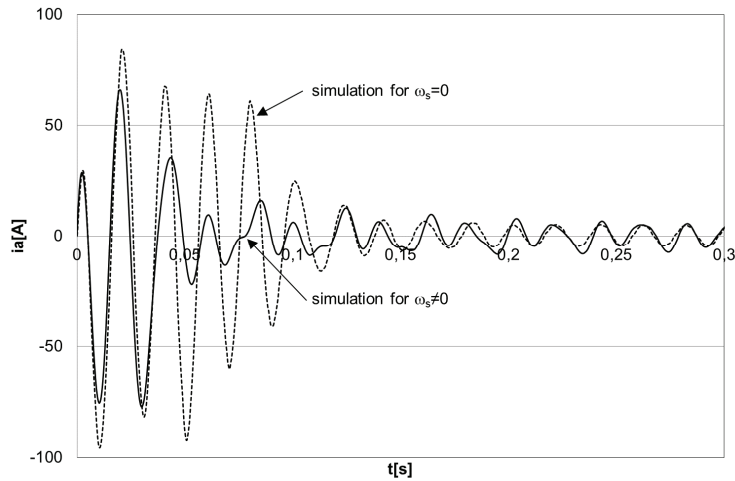


Fig. 12. The comparison of the current waveforms for the double-rotor motor model with one or two mechanical degree of freedom

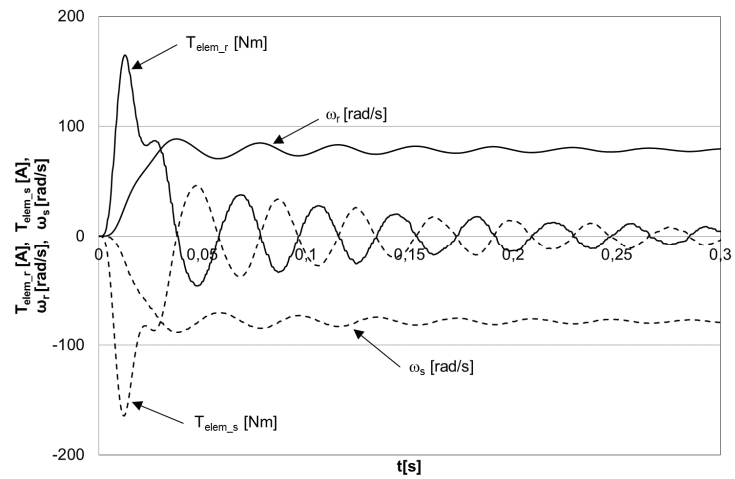


Fig. 13. The simulation of electromagnetic torque acting on the inner and outer rotors and the corresponding angular velocities

The same values were assumed for the inertia moments and the kinetic damping coefficients. Additionally the current waveform has been shown in Fig. 12 assuming that the outer rotor is stationary.

The simulation shows that the torques applied to the rotors have the same waveform, but different signs are oppositely facing each other. The function of the electromagnetic differential is prepared by adding to the system a suitable mechanical transmission driven by the inner rotor. The simulation results also showed that at equal damping, coefficients of a kinetic rotor receives the same speed set but with the opposite signs. The simulation also shows that at equal kinetic damping coefficient the rotor achieves the same steady state values of the angular velocity but with opposite signs. The steady state values of the angular velocity is close to half the synchronous speed of the rotating field. Changes in dynamics of the current, torque and angular velocity of the double-rotor induction motor are other than a single degree of a freedom motor with the same circuit and supply parameters.

6. Conclusions

Based on the experimental and simulation studies it can be concluded that the model of a double rotor induction machine is relatively correct. Its accuracy results from the assumed simplification in the electromagnetic circuit. The results of simulation studies have shown that the electromagnetic torques acting on both rotors have the same waveforms but are oppositely directed assuming the same mechanical properties. On this basis, it can be established that the developed model of the machine can be used in simulations of the electromagnetic differential. The change dynamics of the current, torque and angular velocity of the double-rotor induction motor is other than a single degree of a freedom motor with the same circuit and supply parameters. The comparison of the changing dynamic of the current has shown that in the model with two mechanical degrees of freedom the peak values are lower and disappear quicker. In general it can be concluded that the steady state is achieved faster in a double rotor machine.

References

- [1] Langari R., Won J.-S., *Intelligent energy management agent for a parallel hybrid vehicle-part I: system architecture and design of the driving situation identification process*, IEEE Trans. Veh. Technol., vol. 54, no. 3, pp. 925-934 (2005).
- [2] Larminie J., Lowry J., *Electric vehicle technology explained*, John Wiley & Sons (2003).
- [3] Aripin M.K., Sam Y.Md., Danapalasingam K.A. et al., *A review of active yaw control system for vehicle handling and stability enhancement*, Int. J. Veh. Technol., (2014).
- [4] Han-Wung P., Seok-Gyu O., Young-Joo A., Young-Bae C., Young-Moon H., *Study on double-rotor type driving system for electric vehicle*, Transactions of the Korean Institute of Electrical Engineers, vol. 46, no.1, pp. 46-51 (1997).
- [5] Kelly D.H., *Double-rotor induction motor*, IEEE Transactions on Power Apparatus and Systems, vol. pas-88, no.7, 1086-92 (1969).
- [6] Sobczyk T.J., *Methodological aspects of mathematical modelling of induction machines*, (in Polish), WNT, Warszawa (2004).
- [7] Sobczyk T.J., *On determination of inductances for circuit models of AC machines*, Archives of Electrical Engineering, vol. 62, no. 3, 487-496 (2013).

-
- [8] Sobczyk T.J., Warzecha A., *Estimation of coefficients of multivariable power series approximating magnetic nonlinearity of AC machines*, Archives of Electrical Engineering, vol. 64, no. 3, pp. 379-389 (2015).
- [9] White D.C., Woodson H. H., *Electromechanical energy conversion*, Wiley (1959).
- [10] Cai H., Xu L., *Modeling and Control for Cage Rotor Dual Mechanical Port Electric Machine–Part I: Model Development*, IEEE Transactions on Energy Conversion, vol. 30, no. 3, pp. 957-965, Sept. (2015).
- [11] McCleer P.J., Miller J.M., Gale A.R. et al., *Nonlinear model and momentary performance capability of a cage rotor induction machine used as an automotive combined starter-alternator*, IEEE Transactions on Industry Applications, vol. 37, no. 3, pp. 840-846, May/June (2001).
- [12] Adamczyk D., Wilk A., *Double-rotor induction motor model in electromagnetic differential aspect*, (in Polish), LI International Symposium On Electrical Machines, Electrical Machines – Transaction Journal, no. 4, pp. 37-42 (2015).

